Usefulness of Gadolinium-Enhanced MR Imaging in the Evaluation of the Vascularity of Scaphoid Nonunions

Luis Cerezal[1]
Faustino Abascal[1]
Ana Canga[2]
Roberto García-Valtuille[1]
Manuel Bustamante[3]
Francisco del Piñal[4]

OBJECTIVE. The objective of this article is to identify the role of gadolinium-enhanced MR imaging in the preoperative evaluation of the vascular status of the proximal fragment in scaphoid nonunions.

SUBJECTS AND METHODS. Thirty consecutive patients (27 men and three women; age range, 19–52 years; mean age, 28 years) with nonunion of the scaphoid were prospectively examined with unenhanced and gadolinium-enhanced MR imaging. MR images and surgical findings were classified in four groups according to the vascular status of the proximal fragment (normal bone, moderate ischemic bone, severe ischemic bone, and avascular necrosis). Sensitivity, specificity, and accuracy of unenhanced and gadolinium-enhanced MR studies were calculated. Surgical findings were used as the gold standard. The postoperative rate of union at 12 months was evaluated for each group.

RESULTS. Unenhanced MR imaging showed a global sensitivity of 36%, specificity of 78%, and accuracy of 68% in the preoperative evaluation of the vascular status of the proximal fragment. Correlation with the surgical findings was not statistically significant ($p < 0.149$). Global sensitivity, specificity, and accuracy of gadolinium-enhanced MR imaging were 66%, 88%, and 83%, respectively. Correlation with the surgical findings was good ($p < 0.0001$). Gadolinium-enhanced sequences allowed accurate diagnosis and enabled the creation of prognostic groups having better correlation with surgical findings and postoperative results.

CONCLUSION. Gadolinium-enhanced MR imaging is the most reliable imaging method for investigating the vascularity of the proximal pole in scaphoid nonunions.

The scaphoid is the most commonly fractured bone of the carpus and, considering all injuries to the wrist, is second only to the distal radius [1, 2]. Scaphoid fracture commonly results from a fall on a dorsiflexed hand in young active individuals [3, 4]. Wrist disability is a relatively common problem after scaphoid fractures because of the frequency with which they fail to heal and become nonunions [5]. The reasons for nonunion are multifactorial and include failure to recognize the original injury, inadequate initial treatment, and anatomic and physiologic factors beyond the control of the physician [6]. The decision of the method of treatment is based on the anatomic location of the nonunion, the presence or absence of instability or deformity, and the vascular status of the proximal fragment [7]. The presence of avascular necrosis of the proximal fragment has been shown to be a critical issue in the outcome after operative management of nonunions [5, 6, 8]. Unfortunately, avascular necrosis has been difficult to diagnose accurately. Sclerotic changes of the proximal fragment on conventional radiographs and CT scans have been used to diagnose avascular necrosis; however, different groups of investigators have shown a lack of correlation of proximal pole radiographic sclerosis and avascular necrosis [6, 8, 9]. Bone scintigraphy is sensitive and can reveal early avascular necrosis, but this technique has a low specificity because areas of minor damage or synovitis may give a positive result; furthermore, the spatial resolution of bone scintigrams is low [10].

MR imaging has been reported to be a useful tool to assess accurately the viability of the proximal pole in scaphoid nonunions [6, 9, 11–14]. However, other groups of investigators believe that the clinical significance of MR imaging is questionable and defend surgical inspection, with visualiza-

Received May 4, 1999; accepted after revision June 29, 1999.

Presented at the annual meeting of the American Roentgen Ray Society, San Francisco, April–May 1998.

[1]Department of Radiology, Hospital Mompía, Mompía (Cantabria) 39100, Spain. Address correspondence to L. Cerezal.

[2]Department of Radiology, Hospital Santa Cruz, Liencres (Cantabria) 39120, Spain.

[3]Department of Radiology, University Hospital Marqués de Valdecilla, Santander 39008, Spain.

[4]Unit of Hand Surgery, Hospital Mutua Montañesa, Santander 39012, Spain.

AJR 2000;174:141–149

0361–803X/00/1741–141

tion of the bleeding points being the most accurate method to determine the vascularity of the proximal fragment [10, 15–17].

The role of MR imaging with gadolinium to evaluate the vascular status in scaphoid nonunions has not, to our knowledge, been clearly established. The purpose of this study is to identify the usefulness of gadolinium-enhanced MR imaging in the assessment of the vascularity of the proximal fragment before surgery in scaphoid nonunions.

Subjects and Methods

Thirty consecutive patients with scaphoid nonunions were examined prospectively between March 1996 and January 1998. Twenty-seven patients were men and three were women, ranging in age from 19 to 52 years with an average age of 28 years. Fracture nonunions were defined as fractures with no radiographic evidence of healing at least 6 months from the time of the injury. The fracture site was in the proximal third (n = 9) and the waist (n = 21). The right hand was involved in 16 patients and the left hand in 14; the dominant hand was involved in 21 patients.

MR examinations were performed on a Signa 1.5-T scanner (General Electric Medical Systems, Milwaukee, WI) with paired 3-inch (8-cm) circular coils. Patients underwent scanning in the prone position with the wrist overhead in the isocenter of the magnet, fingers outstretched, and hand positioned flat against volar padding with the coils taped to the wrist.

The MR imaging protocol included sagittal, axial, and coronal T1-weighted spin-echo images with a TR of 500 msec, a TE of 20 msec, a field of view of 10–12 cm, a matrix size of 256 × 224, two excitations, and a slice thickness of 3 mm with a 0.3-mm interslice gap. The parameters for coronal and axial fat-suppressed T2-weighted fast spin-echo imaging were 3000/50 (TR/TE), a field of view of 12–14 cm, a matrix of 256 × 192, one excitation, and a section thickness of 3 mm with a 0.5-mm gap. Finally, fat-suppressed T1-weighted spin-echo images were obtained (500/20) in the coronal and sagittal planes after IV injection of 0.1 mmol per kilogram of body weight of gadodiamide (Omniscan; Nycomed, Oslo, Norway) with the same parameters as conventional T1-weighted sequences.

Signal intensities of the unenhanced MR images were analyzed independently on both T1- and T2-weighted sequences without considering the results of the enhanced images. Based on a modification of the grades of progressive ischemia described by Sakuma et al. [9] and of the classification for the staging of Kienböck's disease by Imaeda et al. [18], proximal fragments were graded as high, iso-, or low signal intensity compared with that of normal carpal bone marrow. Qualitative analysis was performed on MR images at optimal window width and level settings; the peripheral images were excluded from analysis because of partial volume artifact. The use of identical window width and level settings optimized the accuracy of the subjective assessment of changes in signal intensity.

The analyses of the data of both T1- and T2-weighted images were combined and correlated with the severity of the avascular necrosis.

The preoperative MR images were classified into one of four disease groups, which are analogous to the groups used by Green [19] for subjective classification during surgery: normal or good, moderate ischemia, severe ischemia, and avascular necrosis.

Four groups of disease severity were defined according to the signal intensity of the proximal fragment seen on unenhanced T1- and T2-weighted images. Group 1 included images showing normal to slight ischemia, with the proximal fragment appearing isointense compared with the signal intensity of normal carpal bone on T1- and T2-weighted images. Group 2 included images showing moderate ischemia, with the proximal fragment showing slightly low signal intensity on T1-weighted images and homogenous high signal intensity on T2-weighted images. Group 3 included images showing severe ischemia, with the proximal fragment having variably low signal intensity on T1-weighted and heterogeneous signal intensity on T2-weighted images. Group 4 included images showing avascular necrosis or nonviable proximal fragment, with the proximal fragment showing low signal intensity on T1- and homogeneous low signal intensity on T2-weighted images.

We encountered some difficulties in classifying the MR imaging findings. Frequently, the signal intensity changes in the proximal pole of the scaphoid had a patchy and inhomogenous pattern; moreover, we did not observe a relationship between the changes of signal intensity on T1- and T2-weighted images that would allow us to establish the groups of progressive ischemia described by Sakuma et al. [9]. A patient in whom isointensity of the proximal fragment was seen on T1-weighted images and marked low signal intensity was observed on T2-weighted images was included in the group 4.

The gadolinium-enhanced MR images of the four groups were classified subjectively, on the basis of the percentage of enhancement in the proximal pole of the scaphoid, as determined on a combination of sagittal and coronal images.

Group 1 images showed normal to slight ischemia: marked and homogenous enhancement in more than 80% of the volume of the proximal fragment. Group 2 images showed moderate ischemia: patchy enhancement involving 50–80% of the proximal fragment of the scaphoid. Group 3 images showed severe ischemia: patchy enhancement involving 20–50% of the proximal fragment. Group 4 images showed findings ranging from bone with avascular necrosis to nonviable bone: an absence of or less than 20% enhancement.

Surgery was performed in all the patients by an experienced hand surgeon. At the time of operation the scaphoid fragments were inspected by the surgeon for punctate bleeding and bony consistency. Based on the criteria used by Green [19] to establish four surgical groups, the degree of vascularity was assessed for each group: group 1 (normal or good), group 2 (fair), group 3 (poor), and group 4 (none).

Twenty-seven patients underwent autogenous bone grafting and internal fixation using the Herbert screw (Zimmer, Warsaw, IN). Sufficient fixation was achieved at surgery in all patients. Four of these patients in whom gadolinium-enhanced MR imaging showed avascular necrosis (group 4) underwent bone grafting and internal fixation with the Herbert screw. These patients were young and had proximal poles with good bony consistency, although an absence of vascularization was observed at the time of surgery. The three remaining patients with avascular necrosis of the proximal fragment underwent salvage procedures with scaphoid excision, which allowed histologic analysis of the entire proximal pole. One of these patients with avascular necrosis was a manual worker who did not want to risk failure of the bone graft. The other two patients had advanced degenerative wrist disease.

Specimens were preserved in formalin and then processed and analyzed. Criteria used to identify areas of ischemic necrosis included the presence of necrotic adipose tissue in the medullary compartment, the absence of viable osteocytes in lacunae, and degeneration or disruption (or both) of osteons and trabecular architecture.

After surgery, the wrist was immobilized for an average of 7 weeks (range, 4–10 weeks) in a short arm cast. Postoperative follow-up consisted of performing a clinical study and obtaining serial conventional radiographs on a monthly basis.

Our criteria to establish healing were the absence of pain, radiographic evidence of bridging trabeculae of the bone in both sides of the interposed graft, disappearance of the osteotomy lines on conventional radiographs, and no signs of screw loosening [7].

The final diagnoses as documented in the dictated operative report served as the gold standard for this study. Sensitivities, specificities, and accuracies of enhanced and unenhanced MR images were calculated for each group with 95% confidence intervals.

MR images were evaluated by two musculoskeletal radiologists. Discrepancies between the two independent interpretations were resolved in conference. Interobserver variability was assessed using the kappa statistic. The degree of interobserver agreement, which was measured using the kappa statistic, was interpreted on the following scale: 0–0.2, poor; greater than 0.2–0.4, fair; greater than 0.4–0.6, moderate; greater than 0.6–0.8, good; and greater than 0.8–1, very good.

The postoperative rate of union at 12 months was evaluated for each group. Correlation between the enhanced and unenhanced MR groups, the surgical diagnosis, and postoperative outcome was made using the two-tailed Fisher's exact test or the chi-square statistic. A p value of less than 0.05 was regarded as indicative of a statistically significant difference.

The data were calculated and statistically analyzed using software (SPSS; Statistical Package for the Social Sciences, Chicago, IL) for Windows (Microsoft, Redmond, WA).

Results

Surgical Findings

In the patients treated with bone grafting and internal fixation (n = 27), vascularization was observed as normal to good in five patients (18%), fair in 10 (37%), poor in eight (30%), and absent in four (15%).

In the three patients who underwent salvage procedures, the proximal fragment showed complete absence of punctate bleeding points.

Unenhanced MR Imaging and Enhanced MR Imaging Versus Surgical Findings

Sensitivity, specificity, and accuracy of unenhanced MR images were low compared with the surgical findings (Table 1). The correlation was not statistically significant (p < 0.149). However, in the distinction of potentially viable bone (groups 1, 2, and 3) from complete necrosis (group 4) the results were higher, although not statistically significant (p < 0.068).

Avascular necrosis was correctly diagnosed in five patients (true-positive results) and correctly excluded in 17 patients (true-negative results). Two false-negatives and six false-positives resulted from using the unenhanced MR imaging examinations.

Sensitivity, specificity, and accuracy of enhanced MR imaging for the different groups were good compared with the surgical findings (Table 2). Enhanced MR images showed a good correlation with the surgical findings with a strong statistical significance (p < 0.0001).

In the distinction of potentially viable bone (groups 1, 2, and 3) from complete necrosis (group 4), the results were also statistically significant (p < 0.0001).

Avascular necrosis was correctly diagnosed in six patients (true-positive results) and correctly excluded in 22 patients (true-negative results). One false-negative and one false-positive resulted from using the enhanced MR imaging examinations.

Discrepancies in the assessment of the vascularity of the proximal fragment were present in the unenhanced MR images in seven patients and on enhanced MR images in four patients. Interobserver agreement was good for unenhanced MR images (κ = 0.63) and was very good for the enhanced MR images (κ = 0.85).

Unenhanced MR Imaging, Enhanced MR Imaging, and Surgical Findings Versus Healing

Complete healing was achieved in the 20 patients (74.1%) treated with bone grafting and internal fixation using the Herbert screw. Seven patients did not show the criteria of healing proposed by Fernández [7] and were classified as having persistent pseudoarthrosis.

The seven patients with persistent pseudoarthrosis were included in the operative groups of moderate ischemia (n = 1), severe ischemia (n = 2), and necrosis (n = 4). The unenhanced MR images showed normal to slight ischemia (n = 1), moderate ischemia (n = 1), severe ischemia (n = 2), and necrosis (n = 3); and the preoperative enhanced MR images revealed moderate ischemia (n = 1), severe ischemia (n = 2), and necrosis (n = 4).

The rate of successful union within 12 months for the surgical findings was 100% in group 1 (5/5), 90% in group 2 (9/10), 75% in group 3 (6/8) and 0% (0/4) in group 4. For unenhanced MR imaging, the rate was 100% in group 1 (1/1), 88% in group 2 (7/8), 78% in group 3 (7/9), and 56% in group 4 (5/9) and for gadolinium-enhanced MR imaging was 100% in group 1 (6/6), 89% in group 2 (8/9), 75% in group 3 (6/8), and 0% (0/4) in group 4. An absence of gadolinium enhancement was associated with unsuccessful results.

The correlation of unenhanced MR images and results after surgery was not statistically significant (p < 0.209). The correlation of enhanced MR images and postoperative results was highly significant (p < 0.0001).

In the three patients with excision of the proximal pole of the scaphoid, histologic analysis revealed avascular necrosis was present in more than 80% of the quantitative sample. All these patients had long-standing pseudoarthrosis. In two of these patients with advanced degenerative wrist disease, mid carpal arthrodesis was performed; the third patient, who had no degenerative changes, was treated with proximal-row carpectomy. The two patients with degenerative disease of the wrist presented with proximal fragments that were isointense compared with the rest of the carpal bones on T1-weighted sequences and isointense and markedly hypointense on T2-weighted sequences, respectively. In the patient without degenerative wrist changes, the proximal fragment showed low signal intensity on both T1- and T2-weighted images. Unenhanced MR images enabled correct diagnosis in two cases; however, unenhanced MR images of one case were erroneously interpreted as showing normal vascularization to slight ischemia. Gadolinium-enhanced MR images enabled correct diagnosis in all three cases.

TABLE 1 Correlation of Unenhanced MR Imaging Findings and Surgical Findings

Finding	Sensitivity (%)		Specificity (%)		Accuracy (%)	
	Mean	Range	Mean	Range	Mean	Range
Normal appearance	20	1–70	96	77–99	83	64–93
Moderate ischemia	20	3–55	70	45–87	53	34–71
Severe ischemia	37	10–74	72	49–88	63	43–79
Avascular necrosis	71	30–94	73	51–88	73	53–87
Global	36	20–56	78	68–86	68	59–76

TABLE 2 Correlation of Contrast-Enhanced MR Imaging Findings and Surgical Findings

Finding	Sensitivity (%)		Specificity (%)		Accuracy (%)	
	Mean	Range	Mean	Range	Mean	Range
Normal appearance	80	29–98	92	72–98	90	72–97
Moderate ischemia	60	27–86	85	61–96	76	57–89
Severe ischemia	50	17–82	81	58–94	73	53–87
Avascular necrosis	85	42–99	95	76–99	95	76–99
Global	66	47–82	88	80–94	83	75–89

Discussion

Complications arising from scaphoid fractures are common and include delayed union, nonunion, avascular necrosis, deformity or carpal instability, secondary osteoarthritis, carpal tunnel syndrome, and sympathetic dystrophy [7, 19–21]. The significant number of scaphoid fractures in which complications develop can be attributed to the peculiar vascular anatomy of this bone, especially of the proximal pole, which is vulnerable to posttraumatic ischemia and avascular necrosis because of its precarious blood supply.

Gelberman and Menon [22] found that the scaphoid bone receives its vascularization mainly from the radial artery, with the dorsal and volar branches entering through the

A

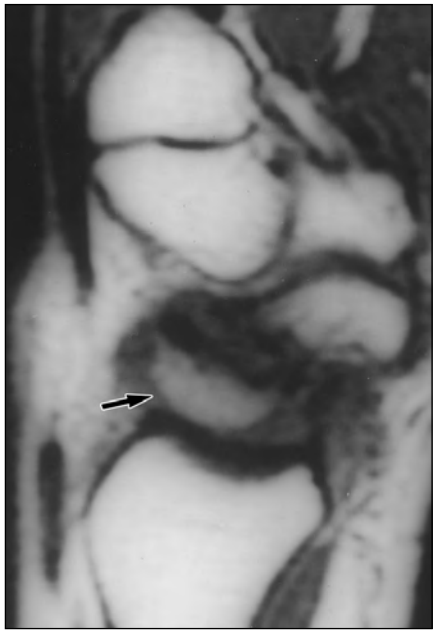

B

C

Fig. 1.—22-year-old man with delayed union. Fracture occurred 11 months earlier.
A, Anteroposterior conventional radiograph shows displaced fracture through waist of scaphoid with sclerosis of proximal fragment.
B, Sagittal T1-weighted spin-echo MR image reveals slight low signal intensity of proximal fragment (*arrow*).
C, Sagittal fat-suppressed T1-weighted MR image obtained with gadolinium shows diffuse enhancement of proximal fragment (*arrow*). Patient healed after surgery.

distal portion of the bone. The vasculature enters the dorsal area of the bone through numerous small foramina along the spiral groove and dorsal ridge. These feeding vessels arise from the dorsal scaphoid branch of the radial artery and the dorsal radial carpal arch. These sources account for approximately 80% of the total blood supply to the scaphoid. The distal area of the bone is supplied with 20% of the total blood supply to the scaphoid by palmar vessels that enter through the tubercle and distal pole. Gelberman and Menon failed to find intraosseus connections between these two areas of blood supply; similarly, they have been unable to show that any significant blood supply enters through the attachments of the scapholunate ligaments. Landsmeer [23] found that the radioscapholunate ligament or ligament of Testut is a neurovascular structure that supplies the scapholunate intraosseous ligament and may vascularize the proximal pole of the scaphoid. Herbert [10] observed numerous patients in whom a small fragment of the proximal pole remained viable when only the scapholunate ligament could have been its source of blood and patients in whom avascular necrosis of the proximal pole occurred after avulsion injuries of the scapholunate ligament without any associated fracture. However, Berger et al. [24] reported that microdissections of cadaver wrists did not reveal any penetration of the vessels into the proximal pole of the scaphoid.

Green [19] reported that although total avascular necrosis was present in only approximately 5–10% of scaphoid fractures, diminished vascularity was usually found. In contrast to the classic concept that avascular necrosis is present in 30% of waist fractures and is almost a certainty in proximal pole fractures [25], Herbert [10] reported that complete avascular necrosis after a fracture, especially if the scapholunate ligament had remained intact, was rare.

Bone grafting with internal fixation is the treatment of choice for scaphoid nonunion, with a success rate of 80–90% [9]. Reasons cited for poor results include the size of the proximal fragment [26], degree of displacement [27], bone grafting method [28], surgical techniques [29, 30], and the presence of avascular necrosis in the proximal fragment, which is the most important factor in predicting the likelihood of success or failure of the surgical treatment in scaphoid nonunions [5, 8].

Gross inspection of the exterior surface of the bone during surgery and of the punctate bleeding points is usually the most important test by which wrist surgeons can assess the vascularity of scaphoid nonunions. Green [8] advocated direct visualization of punctate bleeding in cancellous bone found at surgery as the best determinant of true avascular necrosis because in his experience with 45 scaphoid nonunions treated with Russe bone grafting, union was consistently achieved when bleeding was clearly visible in the proximal pole. Conversely, with a paucity of punctate bleeding, successful union was considerably decreased, and in all cases with a total absence of visible bleeding, nonunion was the rule. Green concluded that if the proximal pole appears nonviable, bone grafting for scaphoid nonunion is likely to fail and an alternative treatment should be considered. Other authors have agreed with Green that visualization of punctate bleeding during surgery is the most accurate method of determining vascularity of the proximal pole [16, 17]. We analyzed this finding with respect to the outcomes in our series. Nevertheless, Green acknowledged the limitations of intraoperative scrutiny of the punctate bleeding points as the sole criterion of avascular necrosis and the need for a more objective and consistently reproducible method of vascular analysis.

Intraoperative biopsy can be misleading because of the patchy pattern of avascular necrosis [31]. Biopsy specimens are likely to contain both viable and dead osteocytes and cannot be used to accurately predict the histologic status of

Fig. 2.—27-year-old man with long-standing pseudoarthrosis, dorsal segmental intercalated instability, synovitis, and advanced degenerative changes in radioscaphoid joint.
A, Coronal T1-weighted sequence shows proximal fragment is isointense to other carpal bones.
B, Fat-suppressed T2-weighted MR image in coronal plane shows marked low signal intensity of proximal fragment (*arrow*).
C, Coronal fat-suppressed T1-weighted MR image with gadolinium shows complete absence of enhancement in proximal fragment (*arrow*). Necrosis of proximal fragment was found at surgery. Resection of necrotic bone and wrist arthrodesis was performed. Histopathologic analysis of bone specimen confirmed necrosis.

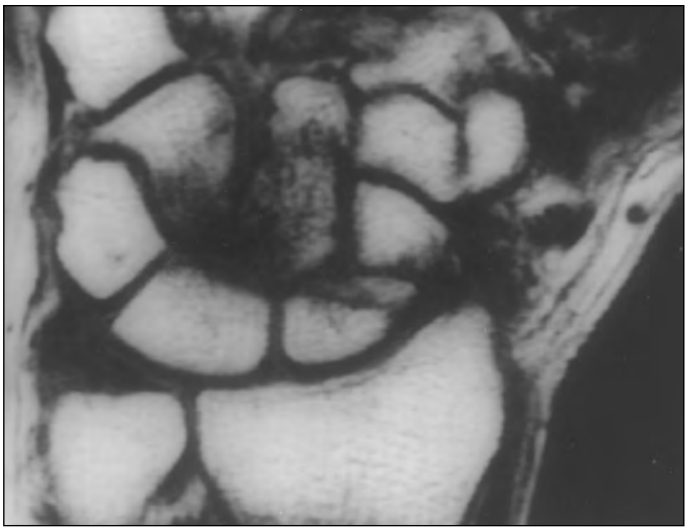

A

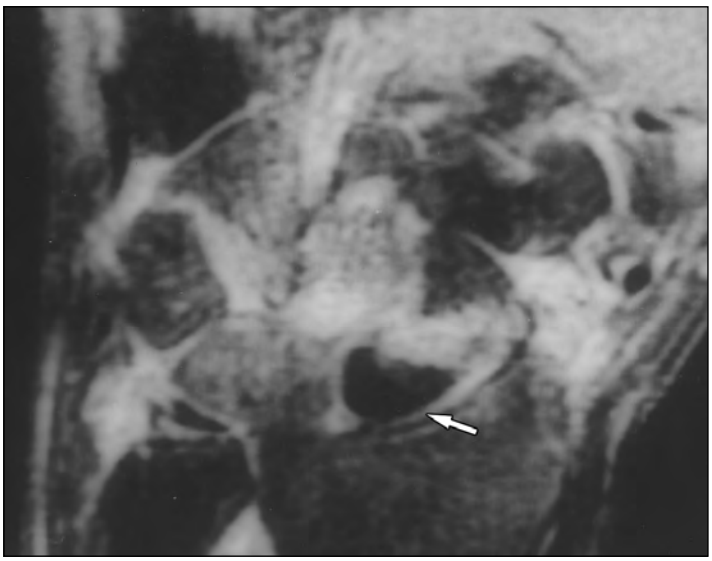

B

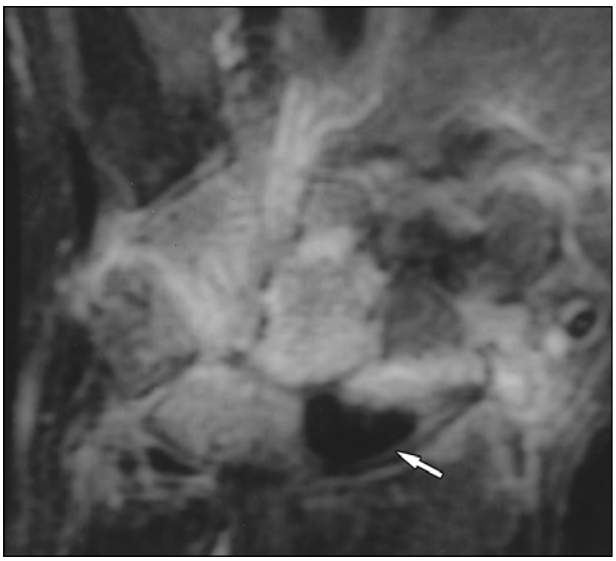

C

the entire fragment; therefore, serial sections of the entire proximal pole would be necessary to prove the existence of complete avascular necrosis [31]. Urban et al. [31] showed how a biopsy specimen from a presumedly avascular scaphoid can be interpreted as viable bone and how a scaphoid with some bleeding in the base of the cancellous bone can be interpreted as avascular. Therefore, findings from random biopsy cannot be used to determine the histologic status of the entire specimen because focal areas of normal-appearing bone may exist adjacent to regions of necrosis. Other methods are necessary to determine scaphoid viability. However, there are not accurate examinations by which to quantify the exact degree of vascularity. Conventional radiography and CT cannot preoperatively predict the amount of avascular necrosis because sclerosis of the proximal fragment does not necessarily correlate with avascular necrosis [6, 8, 9] (Fig. 1). Although bone scintigraphy is very sensitive and can detect early avascular necrosis, this technique has a low specificity. Areas of increased radionuclide activity can be observed wherever there is a posttraumatic healing process, even in the absence of bone ischemia; furthermore, the low spatial resolution of bone scans makes defining the exact area of avascular bone difficult. Toward this end, evidence is accumulating that MR imaging is a suitable technique for noninvasively identifying the vascular status in acute fractures [32] and nonunions [6, 9, 11–14, 25] of the scaphoid and, therefore, can be used as part of the preoperative assessment.

Perlik and Guilford [6] used MR imaging prospectively to predict avascular necrosis in 10 patients with scaphoid nonunion. In their study, MR imaging was found to have an accuracy of 100% compared with an accuracy of only 80% for surgical inspection and 40% for conventional radiography.

Desser et al. [14] published data that indicate MR imaging had a 100% specificity in the diagnosis of avascular necrosis of carpal bones. These researchers noted a difference in sensitivity between T1-weighted (89%) and T2-weighted (55%) images in the detection of carpal avascular necrosis. The lower sensitivity of T2-weighted images may be explained by the inherent lower signal-to-noise ratio. Other groups of researchers have re-

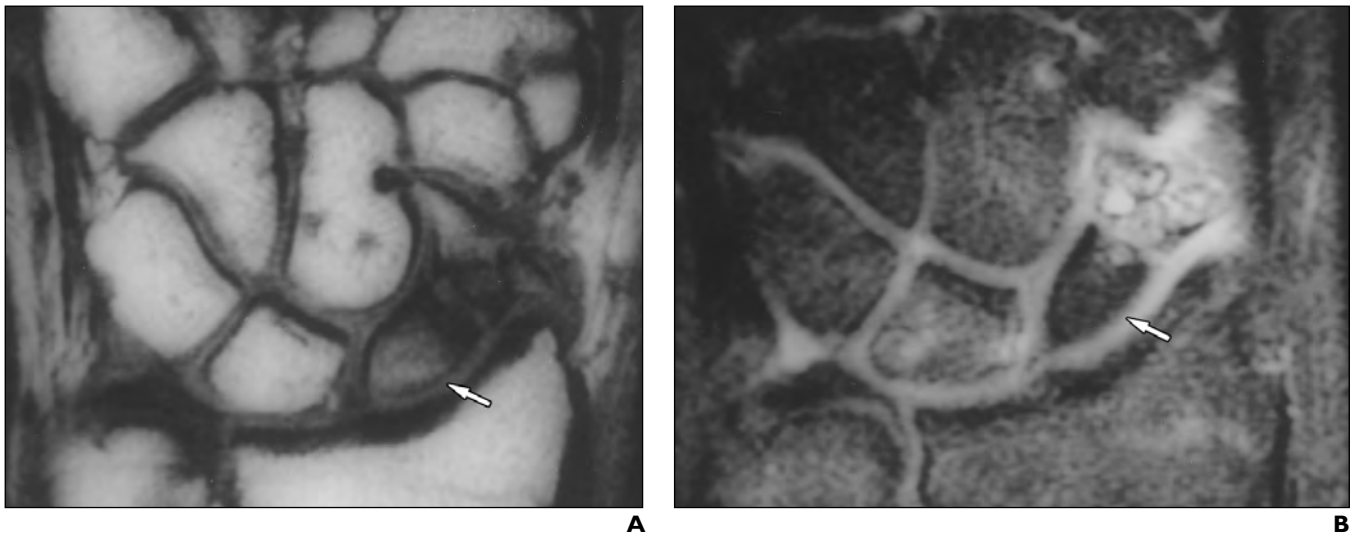

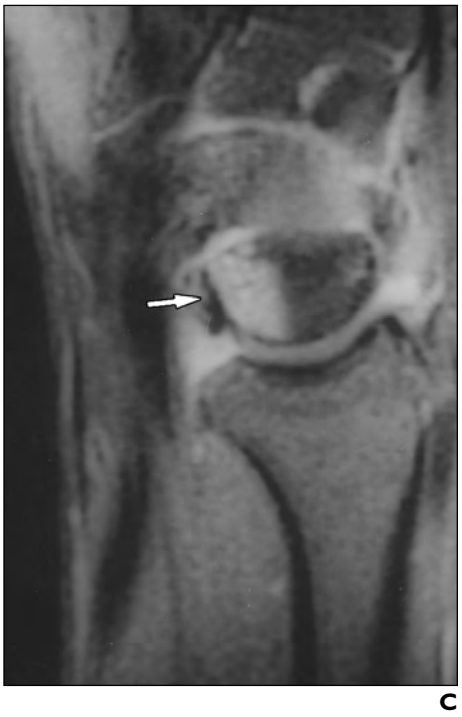

Fig. 3.—31-year-old man with nonunion of scaphoid waist fracture.
A, Coronal T1-weighted MR image shows moderate low signal intensity of proximal fragment (*arrow*).
B, Coronal gadolinium-enhanced fat-suppressed T1-weighted MR image shows absence of enhancement (*arrow*).
C, Sagittal fat-suppressed T1-weighted MR image obtained with gadolinium shows patchy enhancement with viable bone (*arrow*) in palmar aspect of bone and necrosis in dorsal surface. Healing was achieved after surgical treatment with bone grafting and insertion of Herbert screw.

ported that avascular necrosis after scaphoid nonunion was associated with low signal intensity on both T1- and T2-weighted images [9, 11, 13, 14, 25].

However, MR images of scaphoid nonunion are complex and difficult to interpret because in one slice the signal may be diminished or absent, whereas in another slice, the signal may be relatively normal. These findings may reflect the blood supply of the bone because avascularity frequently has a patchwork pattern in which dead osteocytes reside immediately adjacent to viable cells [31].

T1-weighted sequences alone are not useful because in patients in whom normal signal intensity is seen on T1-weighted images, early necrosis with mummified fat is possible, as was seen with three patients in our study (Fig. 2). This finding was described by Vande Berg et al. [33] as affecting the hips of four patients; however, to our knowledge, this finding has not been previously described in the scaphoid. Low signal intensity on T1-weighted sequences does not necessarily mean necrosis; this appearance may just reflect ischemia and potentially viable bone (Fig. 3). Hashizume et al. [34] obtained samples from lunate bones of 10 patients with stage 3 Kienböck's disease and performed histopathologic analysis. Findings from these studies were correlated with MR imaging findings: low-signal-intensity areas seen on MR images did not correlate closely with the extent of the necrotic areas revealed by the histologic findings. In this study, the low-signal-intensity zone on a T1-weighted image was larger than the true necrotic zone and corresponded better with the reactive interface—that is, a distinctive layer of inflammatory and reforming tissue that

Fig. 4.—41-year-old man with long-standing pseudoarthrosis.
A, Coronal T1-weighted MR image shows marked low signal intensity of proximal fragment.
B, Coronal fat-suppressed T2-weighted MR image shows heterogeneous signal intensity of proximal fragment.
C, Coronal gadolinium-enhanced fat-suppressed T1-weighted MR sequence reveals lack of enhancement (*arrow*). No points of punctate bleeding were found at surgery and proximal carpectomy was performed.

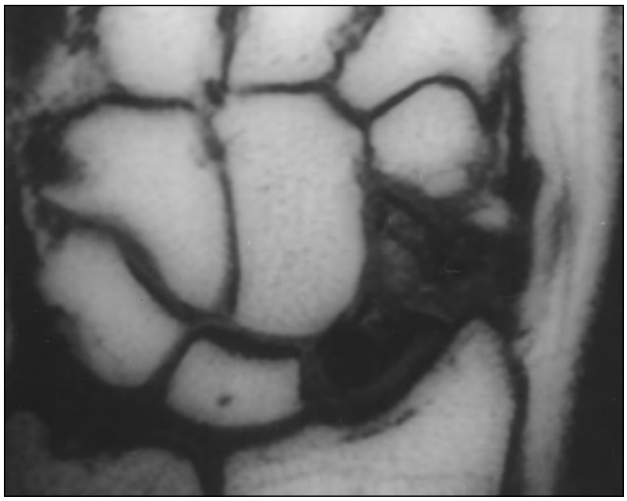

A

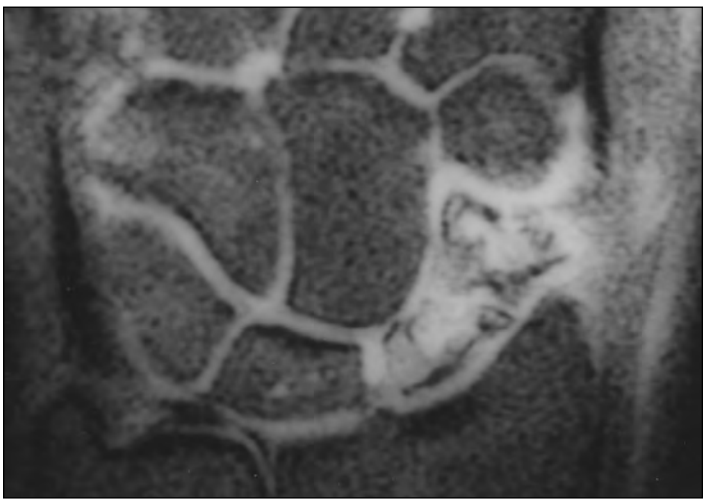

B

C

develops between viable and necrotic bone areas. Therefore, MR imaging exaggerates the necrotic area by showing granulation as having low signal intensity.

Performing T2-weighted sequences did not help much because avascular necrosis may show not only low signal intensity but also normal or high signal intensity and usually has a patchy pattern. Low signal intensity on T2-weighted images usually corresponded with necrosis, but this finding was uncommon in our study.

Inoue et al. [15] refuted the theory that low signal intensity on both T1- and T2-weighted sequences is associated with avascular necrosis and poor results after surgery. These researchers described four patients in whom decreased signal intensity of the proximal fragment was seen on T1- and T2-weighted images and healing was achieved after grafting of cancellous bone and insertion of a Herbert screw.

Moreover, in these studies [6, 9, 11, 13–15] gadolinium was not administered. In our study, when gadolinium was injected, the reduction in blood supply to the proximal fragment could be detected early by comparing the rate of increase in signal intensity after enhancement of the proximal fragment versus that of the normal carpal bones. On T1-weighted fat-suppressed images, the enhancement of hyperemic tissue is easier to see than on spin-echo T1-weighted sequences; the high signal intensity of normal fat is suppressed and only the additional increase in signal intensity caused by vascular perfusion is registered. Under these circumstances, a lack of enhancement of the bone marrow of the proximal scaphoid fragment indicated lack of blood perfusion and therefore variable degrees of ischemia (Figs. 4 and 5).

The signal intensities of the hypervascularized areas in the enhanced MR studies varied from slight to marked low signal intensity on T1-weighted and intermediate to high signal intensity on T2-weighted images.

The unenhanced areas that were individualized on postcontrast images appeared either isointense with fat or hypointense on unenhanced T1-weighted images, and the appearance of these areas was extremely variable on T2-weighted sequences.

The results of our study show that the pattern of signal is frequently patchy and variable on T1- and T2-weighted sequences in both necrotic and viable bone. Unenhanced MR imaging did not allow us to reliably determine the degree of ischemia or viability of the proximal fragment because the correlation of the different groups of ischemia with the surgical groups was poor and an important interobserver variation was seen; however, although inferior to gadolinium-

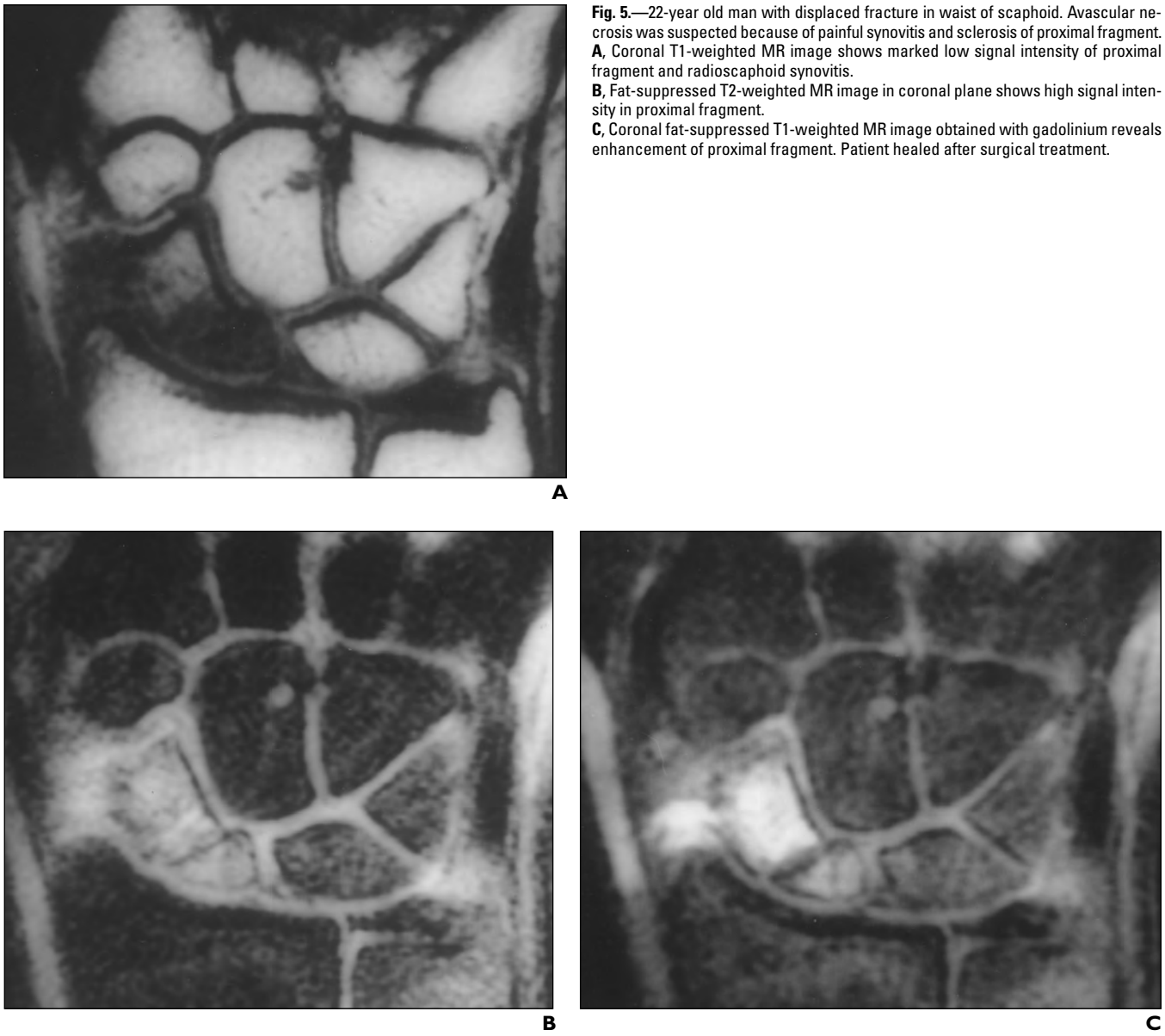

Fig. 5.—22-year old man with displaced fracture in waist of scaphoid. Avascular necrosis was suspected because of painful synovitis and sclerosis of proximal fragment.
A, Coronal T1-weighted MR image shows marked low signal intensity of proximal fragment and radioscaphoid synovitis.
B, Fat-suppressed T2-weighted MR image in coronal plane shows high signal intensity in proximal fragment.
C, Coronal fat-suppressed T1-weighted MR image obtained with gadolinium reveals enhancement of proximal fragment. Patient healed after surgical treatment.

enhanced MR imaging, unenhanced MR imaging enabled us to distinguish between potentially viable bone and nonviable bone.

We propose a new classification system using contrast-enhanced MR imaging to quantify the extent of necrosis of the proximal fragment that in our series showed good correlation with surgical and histologic findings and the healing of the nonunion. We believe that gadolinium-enhanced MR imaging is a good method by which to assess preoperatively the vascular status and healing potential of a given fracture.

One important limitation of our study is that we used the surgeon's impression of the vascularity as the gold standard because there are no other methods by which to quantify the exact degree of vascularity. Nevertheless, the strong statistical significance between the degree of ischemia and the potential of healing suggests that enhanced MR imaging is a reliable exploration by which to determine the vascularization of the scaphoid nonunions. Another limitation is that the rate of enhancement on MR images was subjectively assessed.

From a prognostic standpoint and for the choice of the method of treatment, surgical approach, and type of bone grafting procedure, the clinical decision is based on the anatomic location of the nonunion, the presence or absence of instability or deformity, and the vascular status of the proximal fragment. The first two parameters are clearly diagnosed with conventional radiography and eventually with CT for precise determination of posttraumatic scaphoid deformity [7, 35]. We believe that gadolinium-enhanced MR images are necessary to evaluate accurately the vascular status of the proximal fragment in scaphoid nonunions and can enable the prediction of the healing potential before surgery and help the surgeon select the appropriate surgical procedure. In our opinion, when assessing the degree of vascularity of the proximal fragment, unenhanced MR sequences are not useful and should not be performed, therefore reducing the examination time.

References

1. Larsen CF, Brondum V, Skov O. Epidemiology of scaphoid fractures in Odense, Denmark. *Acta Orthop Scand* **1992**;63:216–218
2. Amadio PC. Scaphoid fractures. *Orthop Clin North Am* **1992**;1:7–17
3. Brondum V, Larsen CF, Skov O. Fracture of the carpal scaphoid: frequency and distribution in a well-defined population. *Eur J Radiol* **1992**;15:118–122
4. Taleisneik J. Fractures of the carpal bones. In: Green DP, ed. *Operative hand surgery,* 2nd ed., vol. 2. New York: Churchill Livingstone, **1988**:813–873
5. Gelberman RH, Wolock BS, Siegel DD. Fractures and nonunions of the carpal scaphoid. *J Bone Joint Surg Am* **1989**;71-A:1560–1565
6. Perlik PC, Guilford WB. Magnetic resonance imaging to assess vascularity of scaphoid nonunions. *J Hand Surg Am* **1991**;16A:479–484
7. Fernández DL. Scaphoid non-union: current approach to management. In: Nakamura R, Linscheid RL, Miura T, eds. *Wrists disorders*. Tokyo: Springer-Verlag, **1992**:153–164
8. Green DP. The effect of avascular necrosis on Russe bone grafting for scaphoid nonunion. *J Hand Surg Am* **1985**;10A:597–605
9. Sakuma M, Nakamura R, Imaeda T. Analysis of proximal fragment sclerosis and surgical outcome of scaphoid non-union by magnetic resonance imaging. *J Hand Surg Br* **1995**;20B:201–205
10. Herbert TJ. *The fractured scaphoid.* St. Louis: Matthew Medical Books, **1990**:13–25
11. Trumble TE. Avascular necrosis after scaphoid fracture: correlation of magnetic resonance imaging and histology. *J Hand Surg Am* **1990**;15A:557–564
12. Morgan WJ, Breen TF, Coumas JM, Schulz LA. Role of magnetic resonance imaging in assessing factors affecting healing in scaphoid nonunions. *Clin Orthop* **1997**;336:240–246
13. Reinus WR, Conway WF, Totty WG, et al. Carpal avascular necrosis: MR imaging. *Radiology* **1986**;160:689–693
14. Desser TS, McCarthy S, Trumble T. Scaphoid fractures and Kienbock's disease of the lunate: MR imaging with histopathologic correlation. *Magn Reson Imaging* **1990**;8:357–361
15. Inoue G, Shionoya K, Kuwahata Y. Ununited proximal pole scaphoid fractures. Treatment with a Herbert screw in 16 cases followed for 0.5-8 years. *Acta Orthop Scand* **1997**;68:124–127
16. Robbins RR, Ridge O, Carter PR. Iliac crest bone grafting and Herbert screw fixation of nonunions of the scaphoid with avascular proximal poles. *J Hand Surg Am* **1995**;20A:818–831
17. Fernandez DL, Eggli S. Non-union of the scaphoid: revascularization of the proximal pole with implantation of vascular bundle and bone grafting. *J Bone Joint Surg Am* **1995**;77-A:883–893
18. Imaeda T, Nakamura R, Miura T, Makino N. Magnetic resonance imaging in Kienböck's disease. *J Hand Surg Br* **1992**;17B:12–19
19. Green DP. Russe technique. In: Gelberrnan RH, ed. *The wrist*. New York: Raven, **1994**:107–118
20. Munk PL, Lee MJ, Logan PM, et al. Scaphoid bone waist fractures, acute and chronic: imaging with different techniques. *AJR* **1997**;168:779–786
21. Duppe H, Johnell O, Lundborg G, Karlsson M, Redlund-Johnell I. Long-term results of fracture of the scaphoid: a follow-up study of more than thirty years. *J Bone Joint Surg Am* **1994**;76-A:249–252
22. Gelberman RH, Menon J. The vascularity of the scaphoid bone. *J Hand Surg Am* **1980**;5A:508–513
23. Landsmeer JMF. *Atlas of anatomy of the hand*. New York: Churchill Livingstone, **1976**:32
24. Berger RA, Kaver JM, Landsmeer JM. Radioscapholunate ligament: a gross anatomic and histologic study of fetal and adult wrists. *J Hand Surg Am* **1991**;16A:350–355
25. Golimbu CN, Firooznia H, Rafii M. Avascular necrosis of carpal bones. *Magn Reson Imaging Clin N Am* **1995**;5:281–303
26. Herbert TJ, Fisher WE. Management of the fractured scaphoid using a new screw. *J Bone Joint Surg Br* **1984**;66-B:114–123
27. Cooney WP, Dobyns JH, Linscheid RL. Nonunion of the scaphoid: analysis of the results from bone grafting. *J Hand Surg Am* **1980**;5A:343–354
28. Cooney WP, Linscheid RL, Dobyns JH, Wood MB. Scaphoid nonunion: role of anterior interpositional bone grafts. *J Hand Surg Am* **1988**;13A:635–650
29. Stark HH, Richard TA, Zemel NP, Ashworth CR. Treatment of ununited fractures of the scaphoid by iliac bone grafts and Kirschner-wire fixation. *J Bone Joint Surg Am* **1988**;70-A:982–991
30. Fernandez DL. Anterior bone grafting and conventional lag screw fixation to treat scaphoid nonunions. *J Hand Surg Am* **1990**;15A:140–147
31. Urban MA, Green DP, Anfdemorte TB. The patchy configuration of scaphoid avascular necrosis. *J Hand Surg Am* **1993**;18A:669–674
32. Kulkarni RW, Wollstein R, Tayar R, Citron N. Patterns of healing of scaphoid fractures: the importance of vascularity. *J Bone Joint Surg Br* **1999**;81-B:85–90
33. Vande Berg B, Malghem J, Labaisse MA, Noel H, Maldague B. Avascular necrosis of the hip: comparison of contrast-enhanced and nonenhanced MR imaging with histologic correlation—work in progress. *Radiology* **1992**;182:445–450
34. Hashizume H, Asahara H, Nishida K, Inoue H, Konishiike T. Histopathology of Kienböck's disease. Correlation with magnetic resonance and other imaging techniques. *J Hand Surg Br* **1996**;21B:89–93
35. Nakamura PT, Horii E, Tanaka Y, Imaeda T, Hayakawa N. Three-dimensional CT imaging for wrist disorders. *J Hand Surg Br* **1989**;14B:53–58

This article has been cited by:

1. Naveen S. Murthy. 2013. The Role of Magnetic Resonance Imaging in Scaphoid Fractures. *The Journal of Hand Surgery* **38**:10, 2047-2054. [CrossRef]
2. Alex W. H. Ng, James F. Griffith, Mihra S. Taljanovic, Alvin Li, W. L. Tse, P. C. Ho. 2013. Is dynamic contrast-enhanced MRI useful for assessing proximal fragment vascularity in scaphoid fracture delayed and non-union?. *Skeletal Radiology* **42**:7, 983-992. [CrossRef]
3. Catherine L. Hayter, Stephanie L. Gold, Hollis G. Potter. 2013. Magnetic resonance imaging of the wrist: Bone and cartilage injury. *Journal of Magnetic Resonance Imaging* **37**:5, 1005-1019. [CrossRef]
4. A. Amador Gil, S. Rico Gala. 2013. Radiología de las fracturas: algo más que un trazo. *Radiología* **55**:3, 215-224. [CrossRef]
5. Martin L. Lazarus. 2013. Imaging of Football Injuries to the Upper Extremity. *Radiologic Clinics of North America* **51**:2, 313-330. [CrossRef]
6. David L. CannonWrist Disorders 3383-3476.e8. [CrossRef]
7. Michael G. Fox, Cree M. Gaskin, A. Bobby Chhabra, Mark W. Anderson. 2010. Assessment of Scaphoid Viability With MRI: A Reassessment of Findings on Unenhanced MR Images. *American Journal of Roentgenology* **195**:4, W281-W286. [Abstract] [Full Text] [PDF] [PDF Plus]
8. Asif SaifuddinThe wrist and hand 145-224. [CrossRef]
9. G. Coblenz, G. Christopoulos, S. Fröhner, K. H. Kalb, R. Schmitt. 2006. Skaphoidfraktur und -pseudarthrose. *Der Radiologe* **46**:8, 664-676. [CrossRef]
10. Peter L. Munk, Mark J. Lee. 2000. Gadolinium-Enhanced MR Imaging of Scaphoid Nonunions. *American Journal of Roentgenology* **175**:4, 1184-1185. [Citation] [Full Text] [PDF] [PDF Plus]